

# Probing Fibril Dissolution of the Repeat Domain of a Functional Amyloid, Pmel17, on the Microscopic and Residue Level

Ryan P. McGlinchey,<sup>†</sup> James M. Gruschus,<sup>†</sup> Attila Nagy,<sup>‡</sup> and Jennifer C. Lee<sup>\*,†</sup>

<sup>†</sup>Laboratory of Molecular Biophysics and <sup>‡</sup>Laboratory of Molecular Physiology, National Heart, Lung, and Blood Institute, National Institutes of Health, Bethesda, Maryland 20892, United States

## Supporting Information

**ABSTRACT:** Pmel17 is a human amyloid involved in melanin synthesis. A fragment of Pmel17, the repeat domain (RPT) rich in glutamic acids, forms amyloid only at mildly acidic pH. Unlike pathological amyloids, these fibrils dissolve at neutral pH, supporting a reversible aggregation–disaggregation process. Here, we study RPT dissolution using atomic force microscopy and solution-state nuclear magnetic resonance spectroscopy. Our results reveal asymmetric fibril disassembly proceeding in the absence of intermediates. We suggest that fibril unfolding involves multiple deprotonation events resulting in electrostatic charge repulsion and filament dissolution.

Amyloids are highly ordered protein aggregates with an unbranched filamentous morphology that have been associated with many human diseases.<sup>1</sup> However, emerging evidence suggests that some amyloids are beneficial serving biological roles.<sup>2</sup> Pmel17 is a functional amyloid involved in melanin synthesis and deposition, which forms intraluminal filaments in melanosomes, membranous organelles in which melanin is synthesized and stored.<sup>3</sup> Pmel17 fibrils are proposed to act as scaffolds to which melanin is deposited and possibly to protect cells by sequestering the reactive chemical intermediates en route to this important pigment.<sup>3a,c</sup>

A fragment of Pmel17 (Figure S1 of the Supporting Information), named the repeat (RPT) domain because of its 10-imperfect repeat sequence of proline, serine, threonine, and glutamic acid residues,<sup>3b</sup> forms amyloid in vitro under mildly acidic conditions (pH 4.5–5.5),<sup>4</sup> typical of the melanosomal pH.<sup>5</sup> Importantly, these fibrils readily dissolve near neutral pH ( $\geq 6$ ),<sup>4</sup> supporting the requirement of the acidic melanosome pH for amyloid assembly and stability. This striking observation suggests that the intra- and/or intermolecular electrostatic charge repulsion created upon deprotonation of specific carboxylic acids (there are 15 Glu residues and 1 Asp) is responsible for dissolution of fibrils.<sup>4b</sup>

This reversibility of RPT aggregation and disaggregation may be a characteristic that defines it as a functional amyloid, because many disease-related amyloids are stable to comparably harsher conditions<sup>6</sup> such as chemical denaturation and protease digestion.<sup>7</sup> Hence, we hypothesized that melanosomal pH may be a natural regulator of RPT fibril formation and if RPT is released and exposed to the neutral cytosolic environment, filaments would dissociate and, thus, maintain their benign nature. To gain further kinetic and structural insights into the

RPT fibril disassembly process, we have employed atomic force microscopy (AFM) and solution-state nuclear magnetic resonance (NMR) spectroscopy as ultrastructural and molecular probes, respectively. In particular, we sought to determine whether during this dissolution process, intermediates or oligomers, putative cytotoxic precursors implicated in disease-related amyloids,<sup>8</sup> are populated.

To monitor fibril disassembly, we diluted preformed RPT fibrils [100  $\mu$ M in 20 mM sodium acetate buffer with 100 mM NaCl (pH 5.0) at 37 °C, agitated at 600 rpm for 4 days, final concentration of  $\sim 5$   $\mu$ M] and deposited them on freshly cleaved mica. AFM images were collected under wet buffer conditions, and long, straight, and unbranched filaments with an average height of  $\sim 4$  nm were found (Figure S2 of the Supporting Information). Consistent with our previous work,<sup>4a,b</sup> washing these fibrils with pH 5.0 buffer yielded no sign of morphological change (Figure 1A), whereas when treated with pH 6.5 buffer, the fibrils begin to dissolve (Figure 1B). Using real-time monitoring, the RPT fibril dissolution process reveals the fragmentation of larger fibrils ( $\geq 300$  nm) followed by the complete disappearance of the smaller fragments on the order of minutes.

Using a method called scanning force kymography (SFK),<sup>9</sup> we examined the directionality of fibril disassembly. By repetitively scanning the cantilever tip along the fibril axis, we assembled images from a single fibril into a kymogram (Figure 1C). A total of 18 individual events were observed using SFK, and the rates of disassembly for most fibrils appear to differ at both ends, implying filament directionality, though a few have similar dissociation rates for both ends (Figure S3 of the Supporting Information). A representative kymogram is shown in Figure 1C with a fast- and slow-dissolving end.

While heterogeneous fibril growth has been shown for amyloids such as amylin, A $\beta$ , and the yeast prion PSI<sup>+</sup>,<sup>10</sup> asymmetric disassembly of a functional amyloid has not been demonstrated until now. The observed fragmentation and variation in dissociation rates could be due to structural polymorphism, where a protein can adopt different self-propagating fibril conformations.<sup>11</sup> This suggestion is possible for RPT because a recent solid-state NMR report revealed that indeed RPT fibrils are polymorphic.<sup>12</sup> Because multiple distinct peptide structures are possible even within a single fibril,<sup>13</sup> both intra- and inter-fibril heterogeneity may occur (Figure S4 of the

Received: October 14, 2011

Revised: November 10, 2011

Published: November 17, 2011

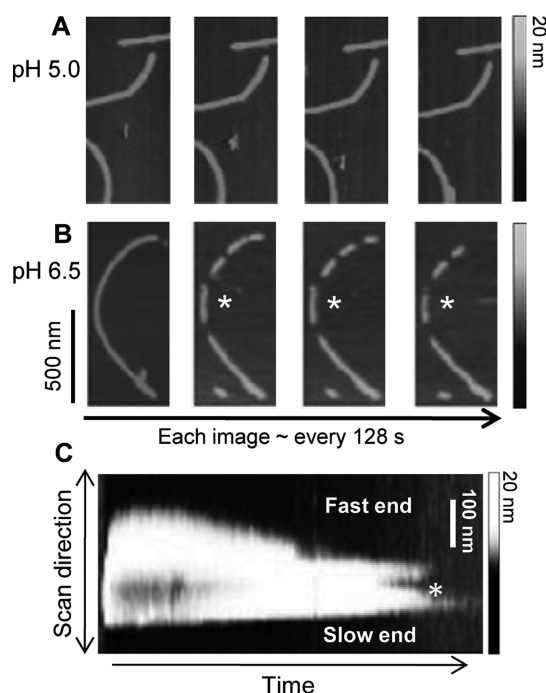


**Figure 1.** Real-time AFM measurements of RPT fibril dissolution. Fibrils formed at pH 5.0 were washed with (A) pH 5.0 or (B) pH 6.5 sodium acetate buffer and monitored over time (an asterisk denotes one disassembly event). Gray scale indicates fibril height. (C) Scanning force kymogram showing a single fibril scanned repetitively along its long axis as a function of scanning time. Ends have been labeled for relative rates (an asterisk denotes fragmentation). Gray scale denotes fibril height. Time scale 0–900 s.

Supporting Information). Another plausible explanation is that there is directional growth of the fibril resulting in distinctive interaction sites at the filament ends.

Despite the presence of heterogeneity, we elected to characterize the kinetics (this rate includes dissolution from both fast and slow ends) by assessing end-to-end filament distances (see Figure 1B). At least 100 individual dissolution events were counted, and an average rate of  $0.16 \pm 0.13$  nm/s was obtained (Figure S4). Because amyloids adopt a cross- $\beta$  structure,<sup>1</sup> where the  $\beta$ -strands in a  $\beta$ -sheet run perpendicular to the fibril axis at an interstrand distance of approximately 0.47 nm, we estimate that on average it would take  $\sim 3$  s to remove these  $\beta$ -strands of each monomer from the fibril.

To gain residue-specific insight into fibril disassembly, we prepared isotopically labeled RPT for NMR spectroscopy. The  $^{15}\text{N}$  HSQC spectrum was first measured for soluble, monomeric RPT at pH 6.5, which provided backbone amide hydrogen and nitrogen resonance assignments for 87 of the 119 non-proline residues, with 29 more being conditionally assigned because of spectral overlap (Figure S5A,C of the Supporting Information). Spectroscopic features (chemical shifts and line widths) of all assigned residues were consistent with the protein adopting a flexible random coil conformation and can be classified as an intrinsically disordered polypeptide.<sup>14</sup>

In the fibrillar state at pH 5.0, no backbone amide resonances were observed for residues 378–444, suggesting that the lack of NMR signal may be due to a large rotational correlation time of the amyloid core (Figure 2 and Figure S5B,D of the Supporting Information). In contrast, resonances for N-terminal residues, 316–377, remain visible albeit with reduced intensities and

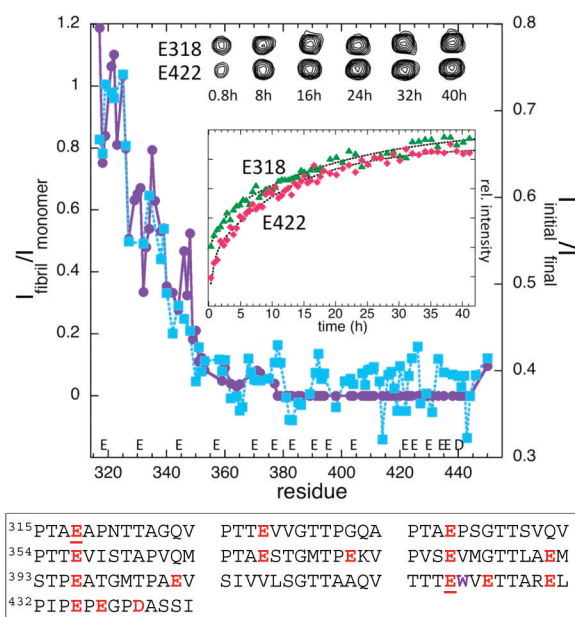


**Figure 2.** Comparison of NMR amide resonance intensities for RPT fibril dissolution (right axis) and fibrillar vs monomer RPT (left axis). Intensity ratios [ $I_{\text{fibril}}/I_{\text{monomer}}$  (purple circles) and  $I_{\text{initial}}/I_{\text{final}}$  (blue squares)] are plotted as a function of residue number for the fibril ( $I_{\text{fibril}}$ , pH 5), monomer ( $I_{\text{monomer}}$ , pH 6.5), initial ( $I_{\text{initial}}$ ), and final ( $I_{\text{final}}$ ) time points of the disassembly process at pH 6.5. The inset shows disassembly kinetics monitored by E318 (green triangles) and E422 (red diamonds) with corresponding resonance peaks at selected times shown above. Acidic residues in RPT are colored red; E318 and E422 are underlined, and W423 is colored purple.

broadened line widths (at least twice that of the monomer), consistent with a reduction in the level of motion compared to that of the monomer, and becoming more immobile as the residues approach the C-terminal region. No chemical shift perturbations were observed ( $<0.03$  ppm); thus, the N-terminal region retains a flexible, unstructured conformation in the amyloid form, nearly indistinguishable from the monomer.

We propose that the RPT fibril core is contained within the C-terminal repeats (residues 378–444). This is consistent with our prior fluorescence study using W423 in repeat 9, which also indicated a key role for the RPT C-terminal region in fibril assembly.<sup>4b</sup> The N-terminal intensity reduction is consistent with restricted motion because of the tethering to the much larger fibril. However, the possibility that some reduction could be due to the incorporation of a subpopulation of the N-terminal residues into the amyloid cannot be ruled out.<sup>12</sup>

To map the RPT disassembly process in detail, we resuspended preformed fibrils in pH 6.5 buffer and recorded a  $^{15}\text{N}$  HSQC spectrum every 30 min up to 42 h at 22 °C. The first spectrum showed 35% recovery of the intensity observed for the monomer spectrum. Subsequent spectra showed a slower, exponential recovery with an average time constant ( $\tau$ ) of 12 h for all residues. The first spectrum appears to be a sum of fibril and monomer spectra, with no evidence of intermediates during the first 30 min. This is shown in Figure 2 via comparison of the intensity ratios of the initial and final spectra to those of the fibril and monomer spectra, which clearly follow the same trend within experimental error.

Though kinetics for every assigned residue were examined, we paid special attention to the Glu backbone amides (Figure S6 of the Supporting Information) because of their implications

in the pH-dependent dissolution process (vide supra). The inset of Figure 2 displays a representative example, showing the backbone amide kinetics of E318 and E422, with E318 positioned outside and E422 within the putative fibril core.<sup>4b</sup> It is clear that there are no significant differences among the different glutamates, suggesting that fibril unfolding is not a local but rather global process involving multiple deprotonation events. Consistent with the spectral data, no intermediate states are apparent as evidenced by the comparable rates, suggesting such states are avoided or are beyond our detection.<sup>15</sup>

The absence of stable oligomeric states during RPT fibril disassembly was also verified using size exclusion chromatography (SEC). RPT fibrils were resuspended in pH 6.5 buffer and directly applied to a pre-equilibrated column. The resulting chromatogram showed two peaks, one of the monomer and the other eluting in the void volume, suggestive of small fibrils with a mass >600 kDa (Figure S7 of the Supporting Information). By preincubation of RPT at pH 6.5 for various lengths of time, it is clear that more monomer is released when the fibrils are exposed for longer time periods, in accord with the NMR results (Figure S7). Our data demonstrate that RPT fibril dissociation is fully reversible because nearly all of the NMR monomer signal intensity is recovered and no apparent stable oligomers are identified by SEC. Nevertheless, further work utilizing other site-specific and highly sensitive probes (e.g., Förster energy transfer) is necessary to delineate the presence of a small population of oligomers.

In summary, we report new structural insights into RPT fibril dissolution. At the microscopic level, fibrils often fragmented before their complete disappearance. In addition, asymmetric dissolution rates were observed. On the residue level, solution-state NMR data identified the amyloid core in the C-terminal region. Moreover, spectral and kinetic data indicate that intermediate states are not populated during dissolution. Because amyloid toxicity has been associated with oligomeric or prefibrillar species that manifest during aggregation and potentially cause membrane disruption,<sup>16</sup> we suggest that in the case of the RPT domain, these events are mitigated because of reversible and pH-dependent amyloid formation.

## ■ ASSOCIATED CONTENT

### ■ Supporting Information

Materials and methods and Figures S1–S7. This material is available free of charge via the Internet at <http://pubs.acs.org>.

## ■ AUTHOR INFORMATION

### Corresponding Author

\*Phone: (301) 496-3741. E-mail: [leej4@mail.nih.gov](mailto:leej4@mail.nih.gov).

### Funding

This work was supported by the Intramural Research Program of the NIH, NHLBI.

## ■ ACKNOWLEDGMENTS

We thank K.-N. Hu for technical assistance and N. Tjandra for use of the 800 MHz NMR spectrometer.

## ■ REFERENCES

- (1) (a) Shewmaker, F., McGlinchey, R. P., and Wickner, R. B. (2011) *J. Biol. Chem.* 286, 16533–16540. (b) Chiti, F., and Dobson, C. M. (2006) *Annu. Rev. Biochem.* 75, 333–366. (c) Jahn, T. R., and Radford, S. E. (2008) *Arch. Biochem. Biophys.* 469, 100–117.
- (2) (a) Fowler, D. M., Koulou, A. V., Balch, W. E., and Kelly, J. W. (2007) *Trends Biochem. Sci.* 32, 217–224. (b) Greenwald, J., and Riek,

- R. (2010) *Structure* 18, 1244–1260. (c) Wasmer, C., Lange, A., Van Melckebeke, H., Siemer, A. B., Riek, R., and Meier, B. H. (2008) *Science* 319, 1523–1526. (d) Chapman, M. R., Robinson, L. S., Pinkner, J. S., Roth, R., Heuser, J., Hammar, M., Normark, S., and Hultgren, S. J. (2002) *Science* 295, 851–855. (e) Balguerie, A., Dos Reis, S., Ritter, C., Chaignepain, S., Coulary-Salin, B., Forge, V., Bathany, K., Lascu, I., Schmitter, J. M., Riek, R., and Saupe, S. J. (2003) *EMBO J.* 22, 2071–2081. (f) McGlinchey, R. P., Yap, T. L., and Lee, J. C. (2011) *Phys. Chem. Chem. Phys.* 13, 20066–20075.
- (3) (a) Berson, J. F., Harper, D. C., Tenza, D., Raposo, G., and Marks, M. S. (2001) *Mol. Biol. Cell* 12, 3451–3464. (b) Hoashi, T., Muller, J., Vieira, W. D., Rouzaud, F., Kikuchi, K., Tamaki, K., and Hering, V. J. (2006) *J. Biol. Chem.* 281, 21198–21208. (c) Fowler, D. M., Koulou, A. V., Alory-Jost, C., Marks, M. S., Balch, W. E., and Kelly, J. W. (2006) *PLoS Biol.* 4, 100–107. (d) Raposo, G., and Marks, M. S. (2007) *Nat. Rev. Mol. Cell Biol.* 8, 786–797. (e) Hurbain, I., Geerts, W. J. C., Boudier, T., Marco, S., Verkleij, A. J., Marks, M. S., and Raposo, G. (2008) *Proc. Natl. Acad. Sci. U.S.A.* 105, 19726–19731.
- (4) (a) McGlinchey, R. P., Shewmaker, F., McPhie, P., Monterroso, B., Thurber, K., and Wickner, R. B. (2009) *Proc. Natl. Acad. Sci. U.S.A.* 106, 13731–13736. (b) Pfefferkorn, C. M., McGlinchey, R. P., and Lee, J. C. (2010) *Proc. Natl. Acad. Sci. U.S.A.* 107, 21447–21452. (c) McGlinchey, R. P., Shewmaker, F., Hu, K. N., McPhie, P., Tycko, R., and Wickner, R. B. (2011) *J. Biol. Chem.* 286, 8385–8393.
- (5) Bhatnagar, V., Anjaiah, S., Puri, N., Darshanam, B. N. A., and Ramaiah, A. (1993) *Arch. Biochem. Biophys.* 307, 183–192.
- (6) (a)  $\beta$ 2 microglobulin fibrils exhibit highly pH sensitive fibril stability. Filaments formed at a very low pH (2 to 3) can dissociate and re-form folded monomers in neutral or basic solution. (b) Platt, G. W., and Radford, S. E. (2009) *FEBS Lett.* 583, 2623–2629. (c) Yamamoto, S., Hasegawa, K., Yamaguchi, I., Goto, Y., Gejyo, F., and Naiki, H. (2005) *Biochim. Biophys. Acta* 1753, 34–43.
- (7) Murphy, R. M. (2002) *Annu. Rev. Biomed. Eng.* 4, 155–174.
- (8) (a) Roychaudhuri, R., Yang, M., Hoshi, M. M., and Teplow, D. B. (2009) *J. Biol. Chem.* 284, 4749–4753. (b) Kostka, M., Hogen, T., Danzer, K. M., Levin, J., Habeck, M., Wirth, A., Wagner, R., Glabe, C. G., Finger, S., Heinzelmann, U., Garidel, P., Duan, W., Ross, C. A., Kretschmar, H., and Giese, A. (2008) *J. Biol. Chem.* 283, 10992–11003. (c) Stefani, M. (2010) *Curr. Protein Pept. Sci.* 11, 343–354. (d) Uversky, V. N. (2010) *FEBS J.* 277, 2940–2953. (e) Sakono, M., and Zako, T. (2010) *FEBS J.* 277, 1348–1358.
- (9) Kellermayer, M. S. Z., Karsai, A., Benke, M., Soos, K., and Penke, B. (2008) *Proc. Natl. Acad. Sci. U.S.A.* 105, 141–144.
- (10) (a) Goldsbury, C., Kistler, J., Aebi, U., Arvinte, T., and Cooper, G. J. S. (1999) *J. Mol. Biol.* 285, 33–39. (b) Blackley, H. K. L., Sanders, G. H. W., Davies, M. C., Roberts, C. J., Tendler, S. J. B., and Wilkinson, M. J. (2000) *J. Mol. Biol.* 298, 833–840. (c) DePace, A. H., and Weissman, J. S. (2002) *Nat. Struct. Biol.* 9, 389–396.
- (11) (a) Petkova, A. T., Leapman, R. D., Guo, Z. H., Yau, W. M., Mattson, M. P., and Tycko, R. (2005) *Science* 307, 262–265. (b) Pedersen, J. S., Andersen, C. B., and Otzen, D. E. (2010) *FEBS J.* 277, 4591–4601. (c) Giraldo, R. (2010) *ChemBioChem* 11, 2347–2357. (d) Kodali, R., Williams, A. D., Chemuru, S., and Wetzel, R. (2010) *J. Mol. Biol.* 401, 503–517.
- (12) Hu, K. N., McGlinchey, R. P., Tycko, R., and Wickner, R. B. (2011) *Biophys. J.* 101, 2242–2250.
- (13) Lewandowski, J. R., van der Wel, P. C. A., Rigney, M., Grigorieff, N., and Griffin, R. G. (2011) *J. Am. Chem. Soc.* 133, 14686–14698.
- (14) (a) Mittag, T., and Forman-Kay, J. D. (2007) *Curr. Opin. Struct. Biol.* 17, 3–14. (b) Wishart, D. S., and Sykes, B. D. (1994) *J. Biomol. NMR* 4, 171–180.
- (15) If intermediate states are manifested in the fibrillar or immobile polypeptide region during the disassembly process, they would not be detectable.
- (16) Uversky, V. N., and Eliezer, D. (2009) *Curr. Protein Pept. Sci.* 10, 483–499.